

Spatial resolution of ballistic electron emission microscopy measured on metal/quantum-well Schottky contacts

C. Tivarus and J. P. Pelz^{a)}

Department of Physics, The Ohio State University, Columbus, Ohio 43210

M. K. Hudait and S. A. Ringel

Department of Electrical and Computing Engineering, The Ohio State University, Columbus, Ohio 43210

(Received 29 June 2005; accepted 6 September 2005; published online 25 October 2005)

Au Schottky contacts on cleaved AlGaAs/GaAs/AlGaAs quantum wells (QWs) were used as precise nanometer-scale apertures to quantify the spatial resolution of ballistic electron emission microscopy (BEEM). Both the amplitude and width of the measured average BEEM current profiles showed systematic dependencies on the QW width and Au film thickness, indicating surprisingly large BEEM resolutions of ~ 12 , ~ 16 , and ~ 22 nm for Au film thicknesses of 4, 7, and 15 nm, respectively, but roughly independent of Au grain size. These measurements are consistent with theoretical models that include multiple hot-electron scattering at interfaces and in the bulk of the metal film. © 2005 American Institute of Physics. [DOI: 10.1063/1.2120899]

Ballistic electron emission microscopy¹ (BEEM) is a method based on scanning tunneling microscopy (STM) that allows the measurement of barrier height at metal/semiconductor and metal/insulator interfaces with nanometric spatial resolution and high energetic precision. Since its development in 1988, the technique has evolved beyond spatially resolved barrier height measurements to include quantitative interface transport characterization, hot-electron (HE) scattering processes in thin metal layers as well as analysis of semiconductor (SC) band-structure and heterostructure band offsets.²

An important technical issue is the spatial resolution of BEEM, since this will ultimately determine how well sample details and closely spaced structures can be resolved. It is also important for fundamental issues of how HEs scatter, spread, and relax in thin metal films. Moreover, the reported high spatial resolution in BEEM measurements has been used in arguments about whether there is lateral momentum conservation of electrons when they cross a metal-SC interface,³ which is a topic still under debate. Several experimental BEEM resolution studies have been done, with a reported BEEM resolution ranging from <2 nm (Refs. 4–8) to several tens of nanometers.⁹ Theoretical studies have also predicted a similarly wide range of BEEM resolution, depending on the assumptions of the models.^{3,6,9–11} However, with one notable exception⁸ the experimental reports of very high spatial resolution were based on the observations of *abrupt changes* to the BEEM current amplitude and/or local Schottky barrier height^{4–7} (SBH) with tip position due to a subsurface structure of unknown origin, or to lithographically defined apertures in an insulating film with significant variations in topographic height and/or lateral dimensions. Such observations must be interpreted with caution, since abrupt changes in the measured properties can also be caused by abrupt changes in the *location* on the STM tip where tunneling occurs when the tip is scanned over a rough surface.¹² It is furthermore difficult to do systematic studies with such unknown and variable structures to determine how BEEM resolution depends on factors such as metal film thickness and grain structure. The exception is the study by

Sirringhaus *et al.*⁸ on an *epitaxial* CoSi₂/Si(111) interface, where the CoSi₂ surface was atomically flat and the subsurface feature was a misfit dislocation or a known structure. In this special case, the almost atomic resolution was explained in terms of focusing effects due to the CoSi₂ band structure and momentum conservation at the epitaxial CoSi₂/Si(111) interface. However, since most BEEM studies involve rough, nonepitaxial polycrystalline metal films, a different approach is desirable that can effectively deal with topography-related artifacts.

In this letter we describe BEEM resolution studies that use cleaved SC quantum wells (QWs) as *nanometer-scale apertures* of well-defined, controllable, and reproducible width. Since the aperture width is essentially constant along the QW (to within ~ 0.3 nm), we could *average together* many “BEEM current profiles” over a QW, to largely remove topography-related artifacts. We then could use *both* the measured *width* and *amplitude* of these average BEEM profiles over the QWs to quantify BEEM resolution, and monitor how this depends on film thickness and metal grain structure. For thin Au films on cleaved GaAs QWs, we found that the lateral BEEM resolution is surprisingly large, ranging from ~ 12 nm for a 4-nm-thick Au film, to ~ 22 nm for a 15-nm-thick Au film. Furthermore, by varying the Au grain size for the same Au thickness, we found that, for our samples, BEEM resolution is roughly independent of the Au grain size.

The samples are ~ 300 -m-diameter Schottky diodes made by Au deposition through shadow masks (metal thicknesses of 4, 7, or 15 nm) on cleaved GaAs QWs (with width ranging from 1 to 15 nm) separated by 200-nm-wide Al_{0.3}Ga_{0.7}As barrier layers. A detailed description of the SC heterostructure and Schottky barrier preparation can be found in Ref. 13. A schematic geometry and wiring for BEEM measurements is shown in Fig. 1(a).

In BEEM, a STM tip held at a voltage ($-V_T$) relative to the thin metal film of a metal-SC structure injects HEs into the structure and a small fraction of injected electrons that have sufficient energy to enter the SC conduction band are “collected” from the SC substrate as the BEEM “collector” current I_C . Figures 1(b) and 1(c), respectively, show a STM topography and a simultaneous “BEEM image” (i.e., a plot

^{a)}Electronic mail: jpelz@mps.ohio-state.edu

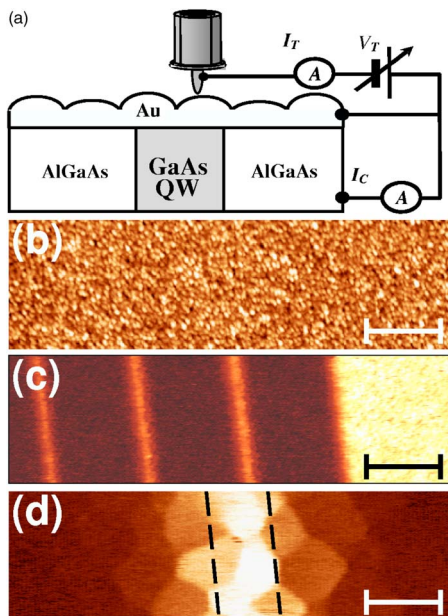


FIG. 1. (Color online) (a) Schematic diagram of sample geometry and wiring for BEEM measurements. (b) STM image of the top 7-nm-thick Au film over a sample region containing (from left to right) the 9, 12, and 15 nm QWs, and wide GaAs reference region (scale bar=150 nm). (c) Simultaneous BEEM image of the same area. (d) Zoom-in image over the 12-nm-wide QW (scale bar=15 nm). The dashed lines show the approximate location of the QW boundaries. Gray scale, 0–4.6 nm for (b) and 0–5 pA for (c) and (d). Data taken with $V_T=1.1$ V and $I_T=15$ nA.

of I_C versus tip position) of a 7-nm-thick Au polycrystalline film located over a sample region with (from left to right) three QWs of widths $d_{QW}=9, 12,$ and 15 nm, and a wide GaAs reference layer. The topographic image shows the granular structure of the polycrystalline Au film, but no discernable features related to the subsurface QWs are seen. In contrast, the BEEM image of Fig. 1(c) clearly reveals the subsurface QWs and the wide GaAs reference layer as regions of enhanced I_C , due to the lower local SBH over the Au/GaAs(QW) regions.¹³ We have found that the SBH $\cong 0.90$ eV for Au/QWs with $d_{QW} \geq 9$ nm is essentially the same as for the Au/GaAs reference layer.¹³ The narrower QWs have increased SBH due to small-size effects¹³ and will not be considered here.

Figure 1(d) shows a zoom-in BEEM image over the 12-nm-wide QW. Notably, enhanced I_C can be seen over a region of more than 50 nm around the QW, much larger than the QW width and approximately five times the size of a typical Au grain. This gives immediate and strong evidence that the lateral spreading of HEs in our 7-nm-thick Au film is much larger than the ~ 1 –2 nm BEEM resolution reported for similar polycrystalline Au films.^{4,6} If BEEM resolution were really ~ 1 –2 nm, then we would expect to clearly observe the edges of the QW in many of the ~ 10 -nm-wide Au grains. Such edges are not seen.

We do, however, observe abrupt variations in I_C amplitude between adjacent Au grains. We believe that these are largely due to two factors: (1) abrupt changes in tunneling location as the tip moves from one grain to another, as discussed in Ref. 12, and (2) grain-to-grain variations in BEEM transmittance that are commonly observed in BEEM measurements on polycrystalline metal films. These grain-related variations in I_C amplitude make it difficult to systematically analyze individual I_C profiles across the QWs. We therefore

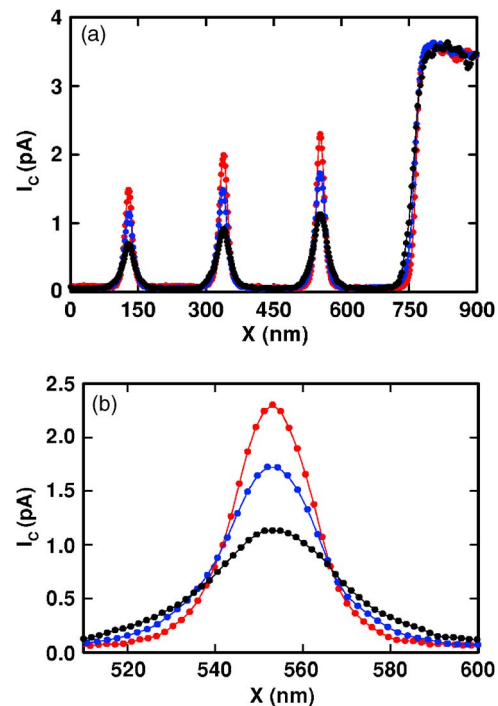


FIG. 2. (Color online) (a) Averaged BEEM profiles over the 9-, 12-, and 15-nm-wide QWs, and the wide GaAs reference region, for three different Au film thicknesses $t_{Au} \cong 4, 7,$ and 15 nm, each measured over a sample region identical to that shown in Figs. 1(b) and 1(c). Since the overall I_C amplitude tends to decrease with increasing film thickness,² these profiles were scaled so that they have the same amplitude over the GaAs reference layer in order to better see systematic dependencies of the profiles on Au film thickness and QW width. There are several important features in these averaged profiles: (1) All profiles over the QWs are *peaked*, and not “flat topped,” as is the profile over the wide GaAs reference region. (2) The full width at half maximum (FWHM) of each peak increases with QW width, and is always significantly larger (by 10–20 nm) than the corresponding QW width [see Fig. 2(b)]. (3) The maximum amplitude of each peak increases with QW width, but in all cases is lower than the amplitude over the reference GaAs region. (4) For each peak, the FWHM *increases* and the peak amplitude *decreases* (relative to the reference GaAs region) with increasing Au film thickness. This can be seen more clearly in Fig. 2(b), which shows a close-up of the three I_C profiles over the 15-nm-wide QW.

consider *averaged* I_C profiles, obtained by averaging data from a BEEM image [e.g., Fig. 1(c)] in a direction parallel to the QWs. This will average out grain-specific local variations in I_C , and leave a reproducible smooth curve representative of the intrinsic I_C profile.

Figure 2(a) shows such averaged BEEM profiles for three different Au film thicknesses $t_{Au} \cong 4, 7,$ and 15 nm, each measured over a sample region identical to that shown in Figs. 1(b) and 1(c). Since the overall I_C amplitude tends to decrease with increasing film thickness,² these profiles were scaled so that they have the same amplitude over the GaAs reference layer in order to better see systematic dependencies of the profiles on Au film thickness and QW width. There are several important features in these averaged profiles: (1) All profiles over the QWs are *peaked*, and not “flat topped,” as is the profile over the wide GaAs reference region. (2) The full width at half maximum (FWHM) of each peak increases with QW width, and is always significantly larger (by 10–20 nm) than the corresponding QW width [see Fig. 2(b)]. (3) The maximum amplitude of each peak increases with QW width, but in all cases is lower than the amplitude over the reference GaAs region. (4) For each peak, the FWHM *increases* and the peak amplitude *decreases* (relative to the reference GaAs region) with increasing Au film thickness. This can be seen more clearly in Fig. 2(b), which shows a close-up of the three I_C profiles over the 15-nm-wide QW.

These features are all easily understood if there exists significant lateral spreading of HEs in the Au film (more than 10–20 nm), which increases strongly with Au film thickness. For example, if the lateral HE distribution for the 4-nm-thick Au film were wider than even the 15-nm-wide QW, then

many of the injected HEs would “miss” the QWs even when the tip is centered over the QW, resulting in a “peaked” maximum with an amplitude that increases with QW width, but is less than the “flat-top” amplitude over the reference GaAs region. Also, if the width of the HE distribution increases strongly with Au film thickness, then all peaks should show a corresponding decrease in peak amplitude (relative to the reference GaAs region), and a corresponding increase in FWHM for thicker Au films. All of this behavior is clearly present in the profiles shown in Fig. 2.

In contrast, most of these features *cannot* be understood if, as previously suggested, HEs are confined to a narrow (1–2 nm) “forward-focused” beam even for a 15-nm-thick Au film. In this case, the peaks over the QWs in Figs. 1 and 2 should have FWHMs which should depend very weakly on Au film thickness and are at most 2–4 nm wider than the corresponding QWs. These peaks should also have relative peak amplitudes that are essentially independent of Au film thickness. This expected behavior is in strong disagreement with the measured profiles in Fig. 2.

Recently, Rakoczy *et al.*¹⁴ reported that the SBH profile (as determined from local BEEM current-voltage spectra) at the GaAs/Al_{0.3}Ga_{0.7}As interface is smeared out over a large lateral distance (approximately tens of nanometers). This behavior was attributed to lateral band-bending effects close to the metal interface, although no supporting numerical simulations were done. We have made similar position-dependent BEEM spectra measurements and found that our measured BEEM spectra are best explained by a *linear superposition* of a Au/GaAs spectrum and a Au/Al_{0.3}Ga_{0.7}As spectrum, with relative amplitudes that depend on the distance between the STM tip and the GaAs/Al_{0.3}Ga_{0.7}As interface. Similar measurements and analysis for a Pt/SiC QW system are discussed in detail in Ref. 15. Furthermore, we have done extensive finite-element calculations of lateral band bending close to the intersection of a GaAs/Al_{0.3}Ga_{0.7}As interface with a metal film,^{13,16} which show that lateral variations of the SBH (i.e., the conduction-band minimum just below the metal-SC interface) are, in fact, confined to within a few nanometers from the GaAs/Al_{0.3}Ga_{0.7}As interface. This is due to strong screening from the nearby metal film. One consequence of this is that two QWs spaced more than a few nanometers apart should behave as two *independent* apertures.

We next use the measured I_C profiles to make quantitative estimates of the BEEM resolution R_B , in analogy with the well-known Rayleigh criterion in optics. We define R_B as the minimum separation at which two adjacent QWs could be positioned such that a “dip” would still be observed in the middle of a BEEM profile across the QWs. We estimated this by superimposing a laterally shifted copy of a particular measured average BEEM profile on the original profile, and finding the minimum shift distance for which a dip (of minimum depth equal to the noise in the BEEM profile) can be observed in the middle of the combined profile. In this way we estimated $R_B \sim 12$ nm for $t_{\text{Au}} \cong 4$ nm, $R_B \sim 16$ nm for $t_{\text{Au}} \cong 7$ nm, and $R_B \sim 22$ nm for $t_{\text{Au}} \cong 15$ nm. We note that these values were essentially independent of the QW used for the analysis, and were approximately equal (to within ~ 1 –2 nm) to $(\text{FWHM} - d_{\text{QW}})$ for a particular QW. The results were reproducible from sample to sample and independent of the particular W or PtIr tips used in our measurements.

Finally, we note that these measured values for R_B are an order of magnitude larger than several early studies that were performed on Au/GaAs or Au/Si samples^{3–7} for reasons that are not clear to us. It could be that those studies were subject to the type of tip artifact described in Ref. 12, or that sample-to-sample differences in the Au film structure or the Au-SC interface have much larger effects on BEEM resolution than previously believed. However, our estimates are well in line with theoretical models that included scattering at the top metal surface⁶ and inside the metal^{9–11} and/or carrier channeling effects due to the metal band structure.¹⁷

Finally, we investigated whether the Au grain size has any effect on the width of the measured I_C profiles, and so, on R_B . For these studies, we prepared several samples with the same metal thickness $t_{\text{Au}} \cong 7$ nm, but different Au grain size by keeping the SC substrate at different temperatures during evaporation. We found that the Au grain size increases from an average of about ~ 10 nm for room temperature deposition to about ~ 18 nm for 100 °C deposition, but the measured average I_C profiles were found to be essentially the same for both Au films. This suggests that, at least for our 7 nm Au films, grain size does not significantly influence R_B .

In summary, we have used cleaved SC QWs to evaluate BEEM resolution for nonepitaxial metal-SC structures. We found an unexpectedly large hot-electron lateral spreading, resulting in estimated resolution ranging from ~ 12 nm for a 4-nm-thick Au film to ~ 22 nm for a 15-nm-thick Au film, independent of the Au grain size. We suggest that previous theoretical models that included scattering at the top metal surface and multiple scattering inside the metal may explain the measured low resolution.

This work was supported by the National Science Foundation (under Grant Nos. DMR-0076362 and DMR-0313468) and by the Semiconductor Research Corporation.

¹W. J. Kaiser and L. D. Bell, Phys. Rev. Lett. **60**, 1406 (1988); **61**, 2368 (1988).

²V. Narayanamurti and M. Kozhevnikov, Phys. Rep. **349**, 447 (2001).

³D. L. Smith, E. Y. Lee, and V. Narayanamurti, Phys. Rev. Lett. **80**, 2433 (1998).

⁴A. A. Talin, R. S. Williams, B. A. Morgan, K. M. Ring, and K. L. Kavanaugh, Phys. Rev. B **49**, 16474 (1994).

⁵H. Palm, M. Arbes, and M. Schulz, Phys. Rev. Lett. **71**, 2224 (1993).

⁶A. M. Milliken, S. J. Manion, W. J. Kaiser, L. D. Bell, and M. H. Hecht, Phys. Rev. B **46**, 12826 (1992).

⁷A. Davies, J. G. Couillard, and H. G. Craighead, Appl. Phys. Lett. **61**, 1040 (1992).

⁸H. Sirringhaus, E. Y. Lee, and H. von Kanel, Phys. Rev. Lett. **74**, 3999 (1995).

⁹C. Manke, Y. Bodschnwinna, and M. Schulz, Appl. Surf. Sci. **117/118**, 321 (1997).

¹⁰L. J. Schowalter and E. Y. Lee, Phys. Rev. B **43**, 9308 (1991).

¹¹M.-L. Ke, R. H. Williams, D. I. Westwood, and B. E. Richardson, Microelectron. Eng. **31**, 195 (1996).

¹²J. P. Pelz and R. H. Koch, Phys. Rev. B **41**, 1212 (1990).

¹³C. Tivarus, J. P. Pelz, M. K. Hudait, and S. A. Ringel, Phys. Rev. Lett. **94**, 206803 (2005).

¹⁴D. Rakoczy, G. Strasser, and J. Smoliner, Appl. Phys. Lett. **86**, 202112 (2005).

¹⁵Y. Ding, K. B. Park, J. P. Pelz, K. C. Palle, M. K. Mikhov, B. J. Skromme, H. Meidia, and S. Mahajan, Phys. Rev. B **69**, 041305 (2004).

¹⁶C. Tivarus, J. P. Pelz, M. K. Hudait, and S. A. Ringel, Proceedings of the 2005 International Conference on Characterization and Metrology for ULSI Technology, March 2005 (unpublished).

¹⁷F. J. Garcia-Vidal, P. L. de Andres, and F. Flores, Phys. Rev. Lett. **76**, 807 (1996).